INTEGRAL EVALUATION OF NEUTRAL ENDOPEPTIDASE INHIBITORS AS POSSIBLE ANTIHYPERTENSIVE AGENTS BY MEANS MOLECULAR MECHANICS, FREE ENERGY CALCULATION AND ADME-TOX PROPERTIES

JUAN A. CASTILLO-GARIT [a], EMILIO LAMAZARES [b], YUDITH CAÑIZARES-CARMENATE [c] AND KAREL MENA-ULECIA [d,e]*

[a]*Unidad de Toxicología Experimental, Universidad de Ciencias Médicas de Villa Clara, Cuba.*
[b]*Universidad de Concepción, Biotechnology and Biopharmaceutical Laboratory, Pathophysiology Department; School of Biological Sciences, Victor Lamas 1290, P.O. Box 160-C, Concepción, Chile.*
[c]*Unit of Computer-Aided Molecular "Biosilico" Discovery and Bioinformatic Research (CAMD-BIR Unit), Facultad de Química y Farmacia, Universidad Central "Marta Abreu" de Las Villas, Santa Clara, Villa Clara, Cuba.*
[d]*Departamento de Ciencias Biológicas y Químicas, Facultad de Recursos Naturales. Universidad Católica de Temuco. Ave. Rudecindo Ortega 02950, Temuco, Chile.*
[e]*Núcleo de Investigación en Bioproductos y Materiales Avanzados (BIOMA), Facultad de Ingeniería, Universidad Católica de Temuco. Ave. Rudecindo Ortega 02950, Temuco, Chile.*

ABSTRACT

The most important mechanisms in the blood pressure regulation, fluid volume and sodium-potassium balance in humans is the renin-angiotensin-aldosterone system (RAAS). This regulatory pathway plays a critical role in modulating cardiac function and vascular tone. An alteration in any of the molecules that make up this system (RAAS) could contribute to the development of arterial hypertension. In this important mechanisms, the neutral endopeptidase, also called Neprilysin (NEP) is the main enzyme for the degradation of natriuretic, therefore, it is essential proteins in controlling blood pressure. In this work, we have used docking methodology, molecular dynamics simulationa and free energy calculations method (MM-PBSA), to comprehensively evaluate the inhibitory behavior of some ligands obteined from consulted literature. The principal results obtained shown these ligands were adequately oriented in the NEP pocket. The Lig783, Lig2177, and Lig3444 compounds were those with better dynamic behavior. The energetic components that contribute to the complex's stability are the electrostatic and Van der Waals components; however, when the ADME-Tox properties were analyzed, we conclude that the best possible anti-hypertensive candidate are Lig783 and Lig3444.

Keywords: *Neprilysin; Docking; Molecular Dynamics; Simulations; MM-PBSA; ADME-Tox*.

1. INTRODUCTION

Neprilysin (NEP), also called Neutral Endopeptidase is the principal enzyme for the degradation of natriuretic into renin-angiotensin-aldosterone system (RAAS)[1]. This protein takes Angiotensin-I (Ang-I) as peptidic substrate to convert it into Angiotensin-1,7 (Ang-1,7)[2,3], which, together with Angiotensin-II (Ang-II), causes vasodilation in cardiac and vascular tissues, and therefore, increases in blood pressure[4,5]. As many authors say, the renin-angiotensin-aldosterone system (RAAS), the most important mechanisms in the regulation of blood pressure, fluid volume and sodium-potassium balance in humans[6–9].

In a normal individual, small elevations of blood pressure produce increases in the renal excretion of sodium and water that tend to normalize the abnormality[10,11]. This phenomenon of pressure natriuresis constitutes a powerful feedback mechanism for long-term control of arterial pressure[12]. In patients with arterial hypertension there are a readjustment and a certain flattening of the pressure natriuresis curve[12], for which higher blood pressure levels are necessary to obtain said natriuretic response, which means there is certain sodium retention[13].

Particularly, the NEP inhibition causes the simultaneous inhibition of the RAAS system in conjunction with vasopeptidases, thus, reducing vasoconstriction, enhancing vasodilation, improving sodium and water balance and, in turn, decreasing peripheral vascular resistance and blood pressure[5], while improving local blood flow within the walls of blood vessels. Therefore, Neprilysin is one of the enzymes with the greatest pharmacological potential in the treatment of cardiovascular and inflammatory diseases[14,15].

Currently several compounds have been developed as NEP inhibitor, such as candoxatril and its successor Ecadotril[16]. It has been shown that these compounds have had specific side effects such as cough, taste disturbances, rashes, or angioneurotic edema[15,16], it is for this reason that new NEP inhibitor molecules are currently being constantly sought for the prevention and remedy of hypertension[17–20].

In previous works, we carried out a study with 133 molecules taken from literature as possible inhibitors of Thermolysin, based on the QSAR-IN methodology[21,22]. This enzyme belongs to the M4 protein family[18], with a structural similarity in the active center with the Neutral Endopeptidase (NEP)[18,20]. From this methodology (QSAR-IN and Virtual screening), we obtained the best six candidates as possible Thermolysin inhibitors (Fig. 1)[22]. In this work we take these six compounds (Fig. 1) to carry out a comprehensive analysis based on molecular mechanics calculations (Docking experiments, Molecular Dynamics Simulation, Free Energy Decomposition energy by means MM-PBSA) and AMDE-Tox properties for proving if these molecules could be good anti-hypertensive agents.

2. COMPUTATIONAL DETAILS

This study starts from a data set composed of six molecules which are represented in Fig. 1[21,22]. These molecules were optimized by means DFT calculations at the *b3lyp/ma-def2-SVP* basis set implemented in Orca 4.2.1 software[23,24]. The full optimized geometry of all molecules were checked by counting their imaginary frequencies. The optimized compounds were used for docking experiments into Neprilysin (NEP) active center.

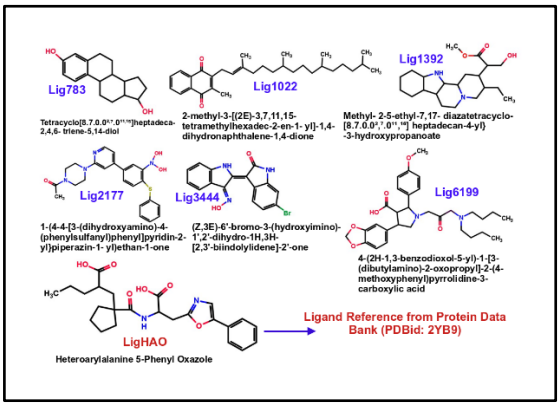

Figure 1. 2D Structural representation of ligands studied in this work as possible NEP inhibitors.

2.1 Docking Experiments.

The X-ray crystallography structure of Neprilisin (NEP) was obtained from Protein Data Bank (PDB)[25,26], whose PDBid is 2YB9, resolved at 2.40 Å[27].

*Corresponding author email: kmena@uct.cl

The protein and ligands were prepared at pH=7.4 using Autodock Tools[28]. For all docking experiment we take the grid box size around the mass centers of the LigHAO (Heteroaryl-alanine-5-phenyl oxazole) in the NEP pocket whose size was 25x25x25 $Å^3$. The grid coordinates were x = 31,959 y=-43,612 and z = 37,509 and zinc atom (Zn^{2+}) was maintained in Neutral Endopeptidase (NEP) active center due to this protein is a metalloprotein of M4 familly[29]. All docking experiments were realized with a grid spacing of 0.375 Å and the number of modes was 10. The energy rank was set up to 1 kcal/mol and to obtain the correct docking pose we realized a re-docking procedure under the same docking protocol of the other compounds, taking as reference ligand the LigHAO using Autodock Vina software version 1.2.3[30,31].

The best docking poses were selected using NEP-ligands binding energy (kcal/mol) and the positional root-mean-square deviation (RMSD)[32,33]. The reproducibility of the docking results was verified by calculating the root-mean-square deviation (RMSD) between our ligands and LigHAO. These calculations were performed by the LigRMSD server 1.0 program[34]. All docking figures were madeusing Pymol software version 1.8[35]. The best energetically favorable poses, the more negative binding energy (kcal/mol), and lowest RMSD of each complex were selected for molecular dynamics simulations, MM-PBSA, and ADME-Tox calculation.

2.2 Molecular Dynamics Simulation.

The best energetically favorable poses selected from docking experiment were submitted to molecular dynamics simulations. Topologies and parameters of the ligands were obtained by the SwissParam web Server[36,37]. Each complex was placed into a water box of 15×15×15 $Å^3$ using the TIP3P water model[38,39]. All molecular dynamics simulations were described using CHARMM36 and CGenFF force field for the NEP enzime and our ligand. All complexes were submitted to 50,000 steps for energy minimization using the conjugated gradient methodology to reduce any close contact, 2.0 ns of equilibration and 50 ns of molecular dynamics simulation at 300 K of temperature using the NAMD 2.13 program[40].

2.3 Free Energy Calculation Method.

We used a computational protocol combining Molecular Dynamics simulation and MM-PBSA[41] (Molecular Mechanics-Poisson–Boltzmann Surface Area) to study NEP-ligand interactions. MM-PBSA calculations were realized using *g_mmpbsa* package version 5.1.2[42]. To carry out this calculation, we extracted the last 500 frames from the 50 ns of molecular dynamics simulation and we computed the free energy decomposition into contributions according to the following equation:

$$\Delta G_{binding} = G_{Complex} - (G_{NEP} - G_{ligand}) \qquad \text{Eq.1}$$

In eq. 1, $G_{complex}$ corresponds to the NEP–ligand complex energy, G_{NEP}, and G_{ligand} is the protein and ligand energy. For the free energy decomposition, it was calculated using the following equation:

$$G_x = G_{Elect} + G_{bond} + G_{vdw} + G_{nonpolar} + G_{polar} \quad \text{Eq. 2}$$

In eq. 2; G_x can be $G_{Complex}$, G_{NEP}, or G_{ligand}; E_{bond} include bond, angle, and dihedral angle. E_{elect} is the electrostatic energy contribution; and E_{vdw} is a Van der Waals energy contribution. The G_{polar} represents the polar free energy contribution, which was calculated using the continuum solvent Poisson-Boltzmann (PB) model included in the APBS (Adaptive Poisson-Boltzmann Solver) software version 1.4.1[43,44]. The non polar free energy was calculated according to the following equation:

$$G_{nonpolar} = \gamma SASA + \beta \qquad \text{Eq. 3}$$

In Eq. 3 γ represent the coefficient related to the solvent surface tension, which, in this work, was 0.0072 kcal/mol/ $Å^2$, SASA represents the solvent-accessible surface area, with an amount of 1.4 Å, and β is a fitting parameter.

2.3 ADME-Tox Properties Calculation.

The ADME-tox are properties related with the absorption, distribution, metabolism, and excretion of a certain compound. In this work we used the full optimized geometry of ligands showed in Fig. 1, which also we computed other physicochemical properties such as molecular weight (MW), octanol/water partition coefficient (cLogP), hydrogen bond acceptor (HBA), hydrogen bond donor (HBD), topological polar surface area (TPSA), and rotatable bond count (RB) respectively using SwissADME web server[45,46]. According to the results obtained from the phycochemical variables described above, we can predict the toxicological properties of our ligands into account the Lipinski[47],Veber[48] and Pfizer 3/75 toxicity empirical rules[49] (Tab. 1). With these results we can predict which of the ligands studied may be potential antihypertensive agents.

Table. 1. Empirical rules for predicting ADME-Tox properties of ligands studied.

Properties	Oral Availability		Toxicity
	Lipinski Rules	Veber Rules	Pfizer 3/75 Rules
Molecular Weight (MW) (Da)	**≤500**	-----	-----
Octanol/Water partition coefficient (cLogP)	≤5	-----	≤3
Hydrogen Bond Acceptor (HBA)	≤10	-----	-----
Hydrogen Bond donor (HBD)	≤5	-----	-----
Topological Polar Surface area (TPSA) ($Å^2$)	-----	≤140	≤75
Rotatable Bond Count (RB)	-----	≤10	-----

3. RESULTS AND DISCUSSION.

To perform a comprehensive analysis of the ligands represented in Fig. 1 with the aim of analyzing which of these molecules could be good anti hypertensive agents, we designed a computational protocol which is shown in Fig. 2.

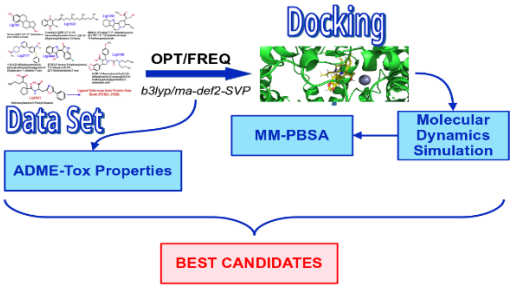

Figure. 2 Sequential computational protocol for the evaluation of possible anti-hypertensive agents studied *in silico*.

The optimized geometry of these molecules was obtained by DFT calculation at the *b3lyp/ma-def2-SVP* basis set and were submitted to Docking experiments into Neutral Endopeptidase pocket. To verify the correct functioning of the docking experiments, we compare our results with the reference ligand heteroarylalanine 5-phenyl oxazole (LigHAO) found in the crystallographic structure of the Neutral Endopeptidase obtained from the Protein Data Bank[25–27], whose PDB id is 2YB9[27].

In this work, we analyzed was whether our docking results reproduced the crystallographic structure obtained from the Protein Data Bank[27]. As shown in Fig. 3, the docked ligand structures had an adequate orientation in the pocket of Neutral Endopeptidase (NEP). It reproduces in an acceptable way the X-ray crystal structure of the NEP-LigHAO complex.

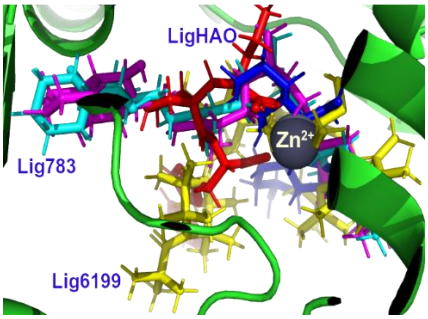

Figure 3. Molecular Docking comparison results of compounds Lig783 (cyan), Lig1022 (magenta), Lig3444 (blue) and Lig6199 (yellow). In red is represented our reference ligand (LigHAO).

Root mean square deviation (RMSD) of the all docket analyzed were calculated taking as our reference ligand (LigHAO) obtained from the Protein Data Bank crystal structure[27]. The values of this parameter (RMSD) are represented in Tab. 2.

Table 2. Calculated binding energies and RMSD of the first ranked Autodock Vina poses for all complexes studied.

Ligand-Protein Complexes	$\Delta G_{binding}$ (kcal/mol) (Rank)	RMSD (Å)	N° H-bond interactions
LigHAO-2YB9	-7.8 (2)	0.245	2
Lig783-2YB9	-7.7 (4)	1.408	1
Lig1022-2YB9	-7.5 (3)	2.012	0
Lig1392-2YB9	-8.0 (1)	1.399	2
Lig2177-2YB9	-8.4 (5)	1.049	4
Lig3444-2YB9	-8.1 (4)	3.334	1
Lig6199-2YB9	-7.9 (7)	1.089	4

As shown, the 57.4% of the poses analyzed had RMSD values below 2.0 Å. This reference RMSD value identifies either correct or incorrect resolution of the docking, RMSD values below 2 were taken into consideration for a correct docking resolution[50,51]. Lig1022, Lig2177 compounds had RMSD values greater than 2 Å, indicating low stability these complexes.

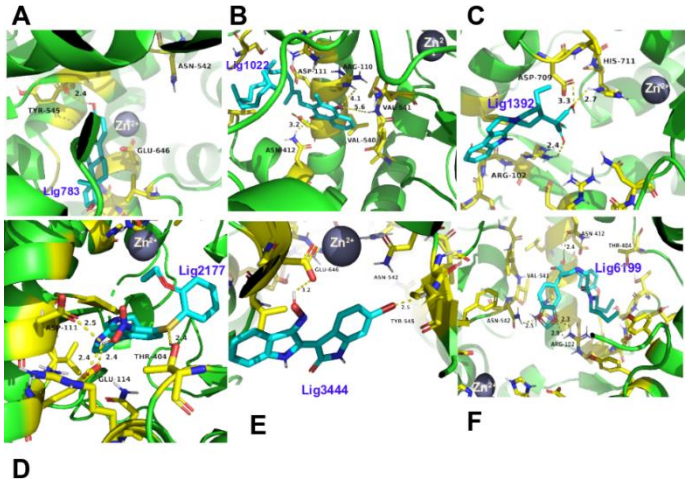

Figure 4. Predicted binding conformations of all investigated complexes from the docking results into NEP Pocket: **(a)** Lig783-2YB9 complex, **(b)** Lig1022-2YB9 complex, **(c)** Lig1392-2YB9 complex, **(d)** Lig11022, **(e)** Lig3444, and **(f)** Lig6199. It is necessary to highlight that Lig1022-2YB9 complex had the least negative binding energy of all the complexes studied and no hydrogen bonding interaction was observed at a distance below 3 Å. This could explain the RMSD value of this complex greater than 2 Å. This result is consistent if we take into account that no hydrogen bond interactions were observed in the neutral endopeptidase active center. This result is consistent if we take into account that no hydrogen bond interactions were observed in the neutral endopeptidase active center. This compound, as shown in Figure 1, has only two hydrogen acceptor groups and a long hydrocarbon chain, which confers hydrophobicity to the ligand, could influence certain steric repulsions within the active center of the NEP, which could be influencing the behavior of this molecule.

To analyze the stability of the studied complexes in the NEP active center, the binding free energy was analyzed. As shown in Tab. 1, all the complexes studied had binding energies more negative than 7 kcal/mol. The most negative $\Delta G_{binding}$ was obtained with Lig2177 ligand (-8.4 kcal/mol). This complex (Lig2177-2YB9) exhibited hydrogen bond interactions with Asp111 (Lig277-OH-O=C-Asp111 to 2.5 Å), Tyr697 (3.33 Å), and Asp709 (3.27 and 2.79 Å). These interactions give this complex certain stability. The second most negative binding energy was found in the complex formed by Lig3444-2YB9 with $\Delta g_{binding}$=-8.1 kcal/mol. The stability of this complex is given by the combination of a hydrogen bond interaction between the N-OH group of the ligand and the carboxyl group of Glu646 and a halogen bond interaction between the bromine (Br) of the ligand and the Tyr545.

Molecular docking experiments give us a criterion of how the ligand interacts in the active site of a given enzyme. To study the complexes dynamic behavior, we have performed molecular dynamics simulations to know if the docking experiments interactions are maintained during the 50 ns of simulation time.

3.1. Molecular Dynamics Simulations complexes behavior

The molecular dynamics simulation method is a very important tool to obtain trajectories that contain all structural information about the stability and relevance of molecular interactions on the ligand-protein complexes and their evolution through time. As a stability criterion, we have quantified the Root-Mean-Square Deviation (RMSD) (Fig. 5)

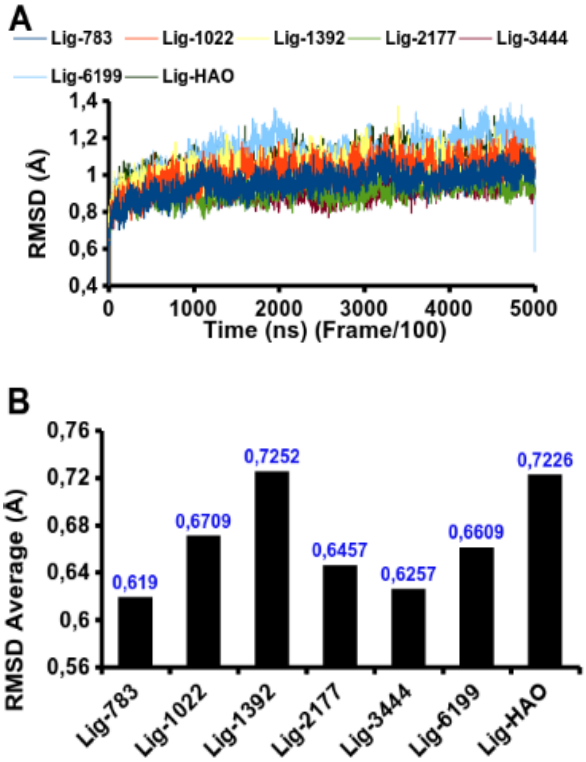

Figure 5. Plots of Root-Mean-Square Deviation (RMSD) parameter against simulation time during 50 ns of molecular dynamics simulations of the studied complexes (A). (B) Average of RMSD for all systems.The less stable complex of all those studied (which does not mean that its behavior is unstable) was Lig1392-2YB9 with an RMSD average value of 0.7252±0.2152 Å, like the complex formed by our reference ligand and the NEP, which had the second-highest RMSD value of all (0.7226±0.2344 Å). Both systems had the two most negative energies in the docking results, indicating that the complexes' dynamic behavior differed from that found in the docking results. To explain this behavior, we will analyze another parameter of these complexes at the molecular level, such as hydrogen bond (H-bond) amount during the simulation time.

As shown in Fig. 6, the complex formed between Lig6199-2YB9 had the most H-bond interactions with an average of 3.00±2.83. Although the number of h-bond interactions was greater than our reference ligand (LigHAO), it is necessary to point out that the stability of these interactions over time was low. The highest occupations were found in the hydrogen bonds formed by Arg114-OE2--HO-Lig6199 (34%) and Arg110-NH--O4-Lig6199 (32%). The other complexes had an average number of h-bond interactions below one with less than 5% occupancy, denoting certain dynamic behavior instability.

This dynamic behavior of this complex (Lig6199-2YB9) was unique since the h-bonds remained stable during the first 25 ns of simulation time, reaching certain instability from nanosecond 26 to 45. From there, it stabilized again until the end of the simulation. This behavior is reflected in the sampling standard deviation, which behaved well above the sample mean.

The second complex with the highest hydrogen bond interaction numbers was Lig783-2YB9. This complex had an average number of h-bond interactions of 2.50±2.12. The dynamics behavior of Lig783-2YB9 was similar to Lig6444-2YB9, in which the hydrogen bonding interactions were not stable over time. Proof of this is that only the interactions between did not exceed an occupancy rate of 40% (Lig783-OH-N-ARG292 occupancy of 36,48% and Gly292-NH-OH-Lig783 of 25,70%).

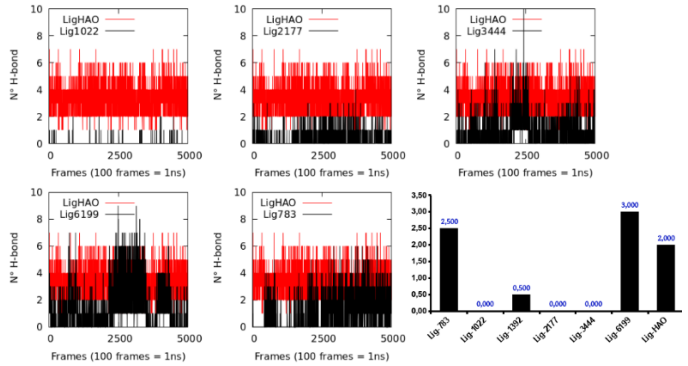

Figure 6. Comparison of the number (and average) of h-bond interactions during 50 ns of simulation time for all complexes studied.

This complex (LigHAO-2YB9), our reference ligand, had the third average number of h-bond interactions (2.00±0.34). This stability over time is due to hydrogen bonds formed by LigHAO-O1--HN-Arg110 and LigHAO-OX--HNArg102 had 100% occupancies. This result indicates the interaction keeping by below 3 Å during the 50 ns of simulation time, our occupation's cutoff parameter. These interactions give the most stablility to this system.

LigHAO-2YB9 and Lig6199-2YB9 were the complexes with the most negative binding energies according to the docking experiments, agrees with the results obtained in this section. However, the RMSD parameter results do not agree with what is shown here. That is why it is necessary to analyze other parameters extracted from the molecular dynamics simulations, such as the radius of gyration and RMSF, which we will display below. The complexes formed by ligands Lig1022, Lig2777 and Lig3444 had the least amount of interactions by hydrogen bonding. Of these, the Lig1022 and Lig3444 were the ones with the fewest hydrogen bonding interactions that were quantified in the docking experiments, which suggests that the stability of these two complexes does not come from hydrogen bonding interactions.

The results analyzed have given a certain degree of agreement between the docking experiments and the h-bond interactions obtained from the trajectories. However, there are discrepancies in the results obtained from the RMSD parameter, so we have to analyze the radius of gyration (Rg), which, is defined as the mean square distance of the atoms set mass with a common mass center[52,53]. With this parameter, we can compare the influence of the compounds on the neutral endopeptidase dynamic behavior.

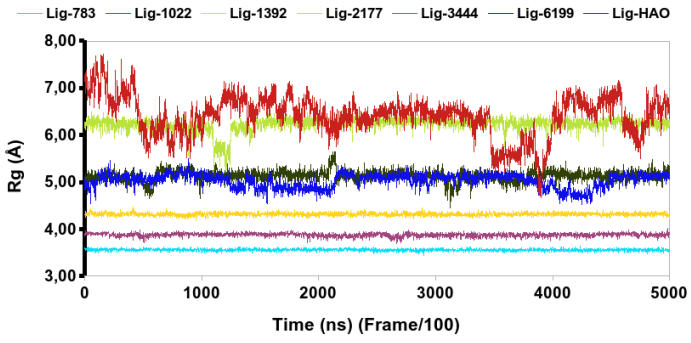

Figure 7. Radius of Gyration (Rg) of all Lig-2YB9 complexes studied during 50 ns of molecular dynamics simulation.

As show in Fig. 7, all the systems studied had Rg values greater than 3.5 Å, higher than other complexes consulted in the literature[54,55]. However, it is necessary to explain why the Lig783-2YB9 and Lig3444-2YB9 complexes had the lowest Rg fluctuation during the 50 ns of molecular dynamics. According to the Rg parameter, the system with the most significant fluctuation was the Lig1022-2YB9. This complex had the least hydrogen bond interaction numbers (Fig. 6). Also, the complexes had the lowest occupancy of these interactions. The highest H-bond interactions occupancy found in this system was formed by Asn542-NH--O-Lig1022 with 0.54%, indicating the instability of this type of interactions, which could explain the Lig1022-2YB9 low degree compaction.

Another of the important parameters to dilute the dynamic behavior of a ligand-protein complex is the Root Means Squared Fluctuation (RMSF). This parameter will help us to observe the flexibility of the amino acids into the neutral endopeptidase pocket in interaction with each of the ligands studied. A high value of RMSF parameter indicates high flexibility, which could be inferred in a more significant movement freedom degree; however, low RMSF values indicate more restricted movements during the molecular dynamics simulation.

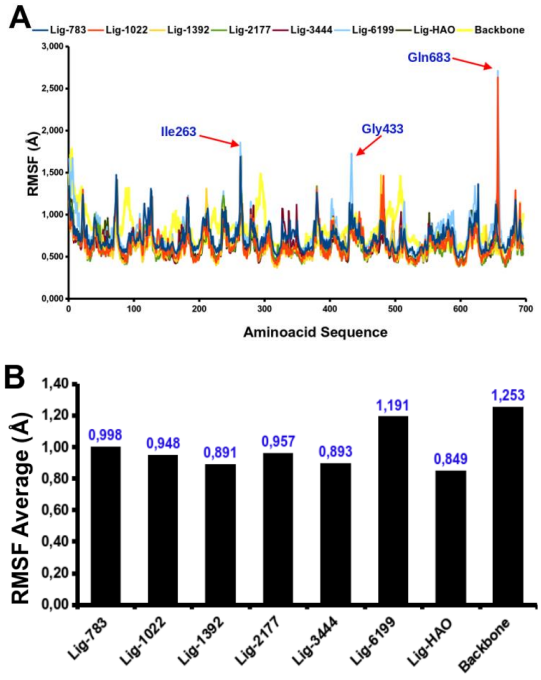

Figure 8. Root Means Squared Fluctuation (RMSF) behavior in the simulation time at 300 Kelvin. (A) RMSF during 50 ns of molecular dynamics simulation. (B) Average of RMSf for all systems studied.

Fig. 8 shows the specific differences between the NEP backbone without ligands and the complexes studied. This difference lies in the greater amino acid flexibility in the absence of ligands. This difference lies in the greater amino acid flexibility in the absence of ligands. However, we observed that the residues between 520 and 670 have the least movement freedom in the backbone (line in yellow in Figure. 7A). Inside this sequence are the amino acids that constitute the NEP pocket (Asn542, His583, Glu584, His587, and Glu646).

The systems studied had lower RMSF values concerning the backbone (Fig. 8B), indicating that the ligands binding with NEP reduces our target protein pocket amino acids flexibility. The complexes formed by the Lig6199, Lig2177 and Lig1022 ligands had the highest RMSF values, which suggest residues more flexible in the NEP active center. This fact explains the Lig1022-2YPB complex behavior when the Rg was analyzed, which was the system with the most fluctuation in this parameter, being the least compact complex of all those studied in this work.

3.2. Molecular Mechanics- Poison-Boltzman Surface Area methods (MM-PBSA)

To determine the energy factors that contribute to the complexes stabilization or destabilization, we have analyzed the energy decomposition using the Molecular Mechanics- Poison-Boltzman Surface Area methods methodology (MM-PBSA)[42,56,57]. The most negative binding energy was obtained by the Lig3444-2YB9 complex ($\Delta G_{binding}$= -78.99±8.67 kcal/mol) (Tab. 3).

This system had the most negative energy in the docking experiments, the second with the lowest RMSD, Rg and RMSF values. This complex has been the most stable of all, considering a comprehensive analysis of the results obtained so far. Our results agree with previous works obtained with this same compound but using another M4 family metalloprotein similar to Neutral Endopeptidase[29,58].

Table. 3. Predicted binding free energies (kcal/mol) and individual energy terms calculated from molecular dynamics simulation through the MM-PBSA methodology.

Complexes	$\Delta G_{binding}$	ΔE_{elec}	ΔE_{vdw}	ΔG_{polar}	ΔG_{apolar}
LigHAO-2YB9	−48,13±16, 22	−157,58±26, 34	−165,39±15,75	296,13±19, 68	−21,27±1,71
Lig783-2YB9	−44,03±12,05	−14,95±10,04	−89,35±11,43	72,10±25, 33	−11,83±1,26
Lig1022-2YB9	−66,32±16,72	0,86±12,31	−129,68 ±17,31	78,69±25,78	−16,19±2,22
Lig1392-2YB9	-45,22±12,95	-25.47±12,76	-69,57±8,25	60,28±11,61	-10,46±0.85
Lig2177-2YB9	−65,64±30,36	−106,32±9,38	−203,96 ±10,13	265,90±24,95	−21,25±0, 80
Lig3444-2YB9	−78,99±18,67	−38,94±23,86	−114,74±11,73	88,19±20,43	−13,45±1,27
Lig6199-2YB9	−71,63±15,62	−44,68±19,86	−127,44±12,48	116,52 ±22,91	−16,03±1,35

Analyzing the free energy decomposition (Tab. 3), we can observe that the electrostatic component, the Van der Waals interactions and the non-polar solvation were the stabilizing contributions of the systems except for the Lig1022-2YB9 complex. In this case, the electrostatic contribution was destabilizing. Considering the H-bond as electrostatic interaction, this complex was the one with the less hydrogen bond numbers in the molecular dynamics simulations and low stability with less than 0.54% of occupancy in all cases analyzed. This fact could be the explanation for the destabilizing positive value of electrostatic energy (ΔE_{elect}).

From Tab. 3 also shown that the Van der Waals term contributes the most to the complex stability, with the most negative energy of all contributions energy calculated using the MM-PBSA method. According to the ligands' structure in this work (Fig. 1) and the docking experiments results (Fig. 4), we can observe that the non-polar hydrocarbon skeletons present attractive hydrophobic interactions with different amino acids in the NEP active center. This approach agrees with the non-polar solvation term results, which positively contributed to the complex's stability studied.

3.3. ADME-Tox Properties

One of the principal aim of this work is to analyze which of all ligands studied are the best candidate as possible anti-hypertensive agents. For this we have calculated the pharmacokinetic (ADME) and toxicological (Tox) properties, considering the Lipinski[47], Veber[48] and Pfizer 3/75[49] empirical rules.

Table 4. Pharmacokinetic (absorption, distribution, metabolism and elimination (ADME)) *in silico* prediction of all ligands studied in this work. In blue we can see compliance and in red non-compliance of empirical rules of Lipinski (LP), Veber (VR) and Pfizer 3/75 (PR) for all the ligands studied.

Properties	LigHAO	Lig783	Lig1022	Lig1392	Lig2177	Lig3444	Lig6199
MW (g/mol)	442,50	272,38	450,70	357,47	480,58	356,17	510,62
cLogP	2,84	2,60	5,86	2,81	3,45	2,31	4,06
HBA	7	2	2	3	5	3	7
HBD	3	2	0	3	2	5	1
RB	12	0	14	5	8	2	13
TPSA (Å^2)	129,73	40,46	31,14	74,35	114,67	76,55	88,54

Ligands		Properties						
			MW (Da)	cLogP	HBA	HBD	TPSA (Å^2)	ER
LigHAO	LP						-	-
	VR		-	-	-	-		
	PR		-		-	-		-
Lig783	LP						-	-
	VR		-	-	-	-		
	PR				-	-		-
Lig1022	LP						-	-
	VR		-	-	-	-		
	PR		-		-	-		-
Lig2177	LP						-	-
	VR		-	-	-	-		
	PR		-		-	-		-
Lig3444	LP						-	-
	VR		-	-	-	-		
	PR		-		-	-		-
Lig6199	LP						-	-
	VR		-	-	-	-		
	PR		-		-	-		-

According to the results shown in Table. 4, we can observe that our reference ligand meets all the contemplated criteria in the Lipinski rule. However, it does not satisfy the rotatable bonds criteria in Veber's rule or the TPSA (Topological Polar Surface Area) criteria from Pfizer's rule. These results indicate that LigHAO is a very flexible molecule and exceeds the polarity range, so we recommend performing experimental tests if this compound is found as a possible anti-hypertensive drug to know if there is a toxicity mechanism.

Of all the compounds designed *in silico*, Lig783 was the only one that agrees with all the parameters contemplated in Lipinski, Veber, and Pfizer's empirical rules, which could be the right candidate for an anti-hypertensive agent. The Lig3444 is another ligand to consider, which complies with all the Lipinski and Veber rule parameters; however, it does not comply with the TPSA parameter like our reference ligand Pfizer Rule. Therefore, it is necessary to be not conclusive with this compound without doing experiments to evaluate the possible toxicity mechanism.

CONCLUSION

Arterial hypertension is one of the health problems that most affect the population worldwide. Given this disease's etiology, hypertensive patients are almost forced to increase the drug dose or change it. Several researchers have been working on designing possible anti-hypertensive agents more effective and reducing as much as possible the side effects that some drugs present on the market. How we know if the compounds designed could be good anti-hypertensive agents?

To answer this question, we successfully applied a sequential computational protocol that provides us, through a comprehensive results analysis, to select which compounds previously designed *in silico* by our group could be good anti-hypertensive agents. Tab. 5 shows a summary of the results obtained through the computational protocol designed for this work, which will help choose the possible anti-hypertensive agents.

Table 5. Comparative summary of the principal results obtained in this work for each computational protocol performed. The numbers represent the ranking compared for each ligand. The plus sign represents the non-violation of the empirical toxicological rules, and the minus sign represents the violation of these rules.

Properties		Lig783	Lig1022	Lig2177	Lig3444	Lig6199
Docking Experiments	$\Delta G_{docking}$	5	2	3	4	1
	RMSD	3	2	5	1	4
Molecular Dynamics Simulation	H-bond	2	5	4	3	1
	RMSD	3	4	1	2	5
	Rg	1	5	4	2	3
MMPBSA	$\Delta G_{binding}$	5	3	4	1	2
ADME-Tox	Lipinski Rules	+	+	+	+	-
	Veber Rules	+	-	+	+	-
	Pfizer 3/75 Rules	+	-	-	-	-

The principal results of this work were that the ligands were oriented adequately in the NEP's active center compared to our reference ligand using the docking experiments. The Lig6199 and Lig1022 ligands had the most negative binding energies of all the complexes studied. However, the lost interactions because of hydrogen bonding from the molecular dynamics analysis of these two complexes (Lig6199-2YB9 and Lig1022-2YB9) caused them to become unstable during the simulation time. The Lig783 and Lig3444 formed the most stable complexes in the molecular dynamics simulations. This result agrees with those obtained in the free binding energy calculations using the MM-GBSA Method which the Lig3444-2YB9 complex had the most negative binding energy. These two ligands could be considered good candidates for anti-hypertensive agents based on the ADME-Tox predictions favorable results. However, this result is not conclusive; first, it is necessary to perform other experimental tests that support our result.

ACKNOWLEDGEMENTS

This work has been supported by Proyecto Interno N°412-5224 from Universidad Católica de Temuco. The authors wish to thank the Universidad Católica de Temuco and Universidad Católica de Santa María for the material and computational facilities.

Powered@NLHPC: This research was partially supported by the supercomputing infrastructure of the NLHPC (ECM-02)

REFERENCES

1. K. Ma, W. Gao, H. Xu, W. Liang, G. Ma, J. Renin-Angiotensin-Aldosterone Syst. JRAAS 2022, 3239057.
2. N. Muñoz-Durango, C. A. Fuentes, A. E. Castillo, L. M. González-Gómez, A. Vecchiola, C. E. Fardella, A. M. Kalergis, Int. J. Mol. Sci. 2016, 17, 797.
3. [L. te Riet, J. H. M. van Esch, A. J. M. Roks, A. H. van den Meiracker, A. H. J. Danser, Circ. Res. 2015, 116, 960.
4. M. A. Elrayess, H. T. Zedan, R. A. Alattar, H. Abusriwil, M. K. A. A. Al-Ruweidi, S. Almuraikhy, J. Parengal, B. Alhariri, H. M. Yassine, A. A. Hssain, A. Nair, M. Al Samawi, A. Abdelmajid, J. Al Suwaidi, M. Omar Saad, M. Al-Maslamani, A. S. Omrani, H. C. Yalcin, Blood Press. 2022, 31, 80.
5. F. R. Mc Causland, M. P. Lefkowitz, B. Claggett, M. Packer, M. Senni, M. Gori, P. S. Jhund, M. M. McGrath, J. L. Rouleau, V. Shi, K. Swedberg, M. Vaduganathan, F. Zannad, M. A. Pfeffer, M. Zile, J. J. V. McMurray, S. D. Solomon, Eur. J. Heart Fail. 2022.
6. M. L. Oliveros-Ruiz, M. Vallejo, C. Lerma, C. Murata, J. Navarro Robles, J. G. Lara, A. De la Peña Díaz, Pregnancy Hypertens. 2022, 27, 117.
7. N. Singhania, S. Bansal, S. Mohandas, D. P. Nimmatoori, A. A. Ejaz, G. Singhania, Drugs Context 2020, 9.
8. H. Wu, T. Y. C. Lam, T. F. Shum, T. Y. Tsai, J. Chiou, Hypertens. Res. 2021 452 2021, 45, 270.
9. K. Trerattanavong, J. (Steven) Chen, StatPearls 2022.
10. S. A. Hubers, N. J. Brown, Circulation 2016, 133, 1115.
11. S. Brown, Vet. Focus 2007, 17, 45.
12. E. J. Baek, S. Kim, Electrolytes Blood Press. E BP 2021, 19, 38.
13. A. E. Vendrov, M. D. Stevenson, A. Lozhkin, T. Hayami, N. A. Holland, X. Yang, N. Moss, H. Pan, S. A. Wickline, J. D. Stockand, M. S. Runge, N. R. Madamanchi, W. J. Arendshorst, Antioxid. Redox Signal. 2022, 36, 550.
14. C. M. Ferrario, L. Groban, H. Wang, X. Sun, J. L. VonCannon, K. N. Wright, S. Ahmad, Kidney Int. Suppl. 2022, 12, 36.
15. Y. Sun, S. Song, Y. Zhang, W. Mo, X. Zhang, N. Wang, Y. Xia, G. Tse, Y. Liu, ESC Heart Fail. 2022, 9, 667.
16. T. Quaschning, F. Ruschitzka, T. F. Lüscher, Curr. Hypertens. Rep. 2002, 4, 78.
17. H. Karimi-Maleh, M. R. Ganjali, P. Norouzi, A. Bananezhad, Mater. Sci. Eng. C 2017, 73, 472.
18. M. C. Fournié-Zaluski, P. Coric, S. Turcaud, N. Rousselet, W. Gonzalez, B. Barbe, I. Pham, N. Jullian, J. B. Michel, B. P. Roques, J. Med. Chem. 1994, 37, 1070.
19. I. Gomez-Monterrey, S. Turcaud, E. Lucas, L. Bruetschy, B. P. Roques, M. C. Fournié-Zaluski, J. Med. Chem. 1993, 36, 87.
20. P. Perrone-Filardi, S. Paolillo, P. Agostoni, C. Basile, C. Basso, F. Barillà, M. Correale, A. Curcio, M. Mancone, M. Merlo, M. Metra, S. Muscoli, S.

Nodari, A. Palazzuoli, R. Pedrinelli, R. Pontremoli, M. Senni, M. Volpe, C. Indolfi, G. Sinagra, Eur. J. Intern. Med. 2022.
21. Y. Cañizares-Carmenate, K. Mena-Ulecia, D. MacLeod Carey, Y. Perera-Sardiña, E. W. Hernández-Rodríguez, Y. Marrero-Ponce, F. Torrens, J. A. Castillo-Garit, Mol. Divers. 2022, 26, 1383.
22. Y. Cañizares-Carmenate, K. Mena-Ulecia, Y. Perera-Sardiña, F. Torrens, J. A. Castillo-Garit, Arab. J. Chem. 2019, 12, 4861.
23. F. Neese, WIREs Comput. Mol. Sci. 2018, 8, e1327.
24. F. Neese, F. Wennmohs, U. Becker, C. Riplinger, J. Chem. Phys. 2020, 152, 224108.
25. H. M. Berman, J. Westbrook, Z. Feng, G. Gilliland, T. N. Bhat, H. Weissig, I. N. Shindyalov, P. E. Bourne, Nucleic Acids Res. 2000, 28, 235.
26. S. Velankar, S. K. Burley, G. Kurisu, J. C. Hoch, J. L. Markley, In Structural Proteomics: High-Throughput Methods (Ed.: Owens, R. J.), Springer US, New York, NY, 2021, pp. 3–21.
27. M. S. Glossop, R. J. Bazin, K. N. Dack, D. N. A. Fox, G. A. MacDonald, M. Mills, D. R. Owen, C. Phillips, K. A. Reeves, T. J. Ringer, R. S. Strang, C. A. L. Watson, Bioorg. Med. Chem. Lett. 2011, 21, 3404.
28. G. M. Morris, R. Huey, W. Lindstrom, M. F. Sanner, R. K. Belew, D. S. Goodsell, A. J. Olson, J. Comput. Chem. 2009, 30, 2785.
29. D. MacLeod-Carey, E. Solis-Céspedes, E. Lamazares, K. Mena-Ulecia, Saudi Pharm. J. 2020, 28, 582.
30. O. Trott, A. J. Olson, J. Comput. Chem. 2010, 31, 455.
31. M. R. Koebel, G. Schmadeke, R. G. Posner, S. Sirimulla, J. Cheminformatics 2016, 8, 27.
32. E. A. Coutsias, M. J. Wester, J. Comput. Chem. 2019, 40, 1496.
33. F. Sapundzhi, M. Popstoilov, M. Lazarova, In Numerical Methods and Applications (Eds.: Georgiev, I.; Datcheva, M.; Georgiev, K.; Nikolov, G.), Springer Nature Switzerland, Cham, 2023, pp. 279–288.
34. J. L. Velázquez-Libera, F. Durán-Verdugo, A. Valdés-Jiménez, G. Núñez-Vivanco, J. Caballero, Bioinformatics 2020, 36, 2912.
35. M. A. Lill, M. L. Danielson, J. Comput. Aided Mol. Des. 2011, 25, 13.
36. V. Zoete, M. A. Cuendet, A. Grosdidier, O. Michielin, J. Comput. Chem. 2011, 32, 2359.
37. A. Waterhouse, M. Bertoni, S. Bienert, G. Studer, G. Tauriello, R. Gumienny, F. T. Heer, T. A. P. De Beer, C. Rempfer, L. Bordoli, R. Lepore, T. Schwede, Nucleic Acids Res. 2018, 46, W296.
38. S. Boonstra, P. R. Onck, E. van der Giessen, J. Phys. Chem. B 2016, 120, 3692.
39. J. Lu, Y. Qiu, R. Baron, V. Molinero, J. Chem. Theory Comput. 2014, 10, 4104.
40. J. C. Phillips, R. Braun, W. Wang, J. Gumbart, E. Tajkhorshid, E. Villa, C. Chipot, R. D. Skeel, L. Kalé, K. Schulten, R. Brauna, W. Wang, J. Gumbart, E. Tajkhorshid, E. Villa, C. Chipot, R. D. Skeel, L. Kale, J. C. Phillips, K. Schulten, J. Comput. Chem. 2005, 26, 1781.
41. S. Genheden, U. Ryde, Expert Opin. Drug Discov. 2015, 10, 449.
42. R. Kumari, R. Kumar, A. Lynn, J. Chem. Inf. Model. 2014, 54, 1951.
43. W. Im, D. Beglov, B. Roux, Comput. Phys. Commun. 1998, 111, 59.
44. J. Wagoner, N. A. Baker, J. Comput. Chem. 2004, 25, 1623.
45. A. Daina, O. Michielin, V. Zoete, Sci. Rep. 2017, 7, 42717.
46. B. Bakchi, A. D. Krishna, E. Sreecharan, V. B. J. Ganesh, M. Niharika, S. Maharshi, S. B. Puttagunta, D. K. Sigalapalli, R. R. Bhandare, A. B. Shaik, J. Mol. Struct. 2022, 1259, 132712.
47. C. A. Lipinski, F. Lombardo, B. W. Dominy, P. J. Feeney, Adv. Drug Deliv. Rev. 2001, 46, 3.
48. D. F. Veber, S. R. Johnson, H.-Y. Cheng, B. R. Smith, K. W. Ward, K. D. Kopple, J. Med. Chem. 2002, 45, 2615.
49. J. D. Hughes, J. Blagg, D. A. Price, S. Bailey, G. A. DeCrescenzo, R. V. Devraj, E. Ellsworth, Y. M. Fobian, M. E. Gibbs, R. W. Gilles, N. Greene, E. Huang, T. Krieger-Burke, J. Loesel, T. Wager, L. Whiteley, Y. Zhang, Bioorg. Med. Chem. Lett. 2008, 18, 4872.
50. H. Gohlke, M. Hendlich, G. Klebe, J. Mol. Biol. 2000, 295, 337.
51. D. B. Kitchen, H. Decornez, J. R. Furr, J. Bajorath, Nat. Rev. Drug Discov. 2004, 3, 935.
52. M. Yu. Lobanov, N. S. Bogatyreva, O. V. Galzitskaya, Mol. Biol. 2008, 42, 623.
53. M. A. Abramowicz, J. C. Miller, Z. Stuchlík, Phys. Rev. D 1993, 47, 1440.
54. K. M. Kumar, A. Anbarasu, S. Ramaiah, Mol. Biosyst. 2014, 10, 891.
55. P. Lavanya, S. Ramaiah, A. Anbarasu, J. Cell. Biochem. 2016, 117, 542.
56. B. Kuhn, P. Gerber, T. Schulz-Gasch, M. Stahl, J. Med. Chem. 2005, 48, 4040.
57. T. Tuccinardi, Expert Opin. Drug Discov. 2021, 16, 1233.
58. E. Lamazares, D. MacLeod-Carey, F. P. Miranda, K. Mena-Ulecia, Molecules 2021, 26, 386.